water

MDPI

Article

Multi-Parameter Algorithms of Remote Sensing Reflectance, Absorption and Backscattering for Coastal Waters of the Southern Baltic Sea Applied to Pomeranian Lakes

Barbara Lednicka [1], Maria Kubacka [2,*], Włodzimierz Freda [1], Kamila Haule [1], Dariusz Ficek [3] and Maciej Sokólski [4]

[1] Physics Department, Gdynia Maritime University, Ul. Morska 81-87, 81-225 Gdynia, Poland; b.lednicka@wm.umg.edu.pl (B.L.); w.freda@wm.umg.edu.pl (W.F.); k.haule@wm.umg.edu.pl (K.H.)
[2] Department of Operational Oceanography, Maritime Institute, Gdynia Maritime University, Ul. Długi Targ 41/42, 80-830 Gdańsk, Poland
[3] Institute of Biology and Earth Sciences, Pomeranian University in Słupsk, Ul. Arciszewskiego 22A, 76-200 Słupsk, Poland; dariusz.ficek@apsl.edu.pl
[4] Institute of Oceanology, Polish Academy of Sciences, Ul. Powstańców Warszawy 55, 81-712 Sopot, Poland; sokol@iopan.pl
* Correspondence: mkubacka@im.umg.edu.pl

Abstract: The Pomeranian lakes in Northern Poland and the nearby coastal waters of the Baltic Sea belong to optically complex water bodies characterised by high eutrophication levels. These water types require a local approach when developing bio-optical algorithms that combine the inherent and the apparent properties of seawater. Well-established local algorithms are of great value for understanding and addressing rapid changes in water quality related mostly to human activities in coastal and near-shore zones, as well as in optically similar lakes. Our research analyses the possibility of using the multi-parameter algorithms of absorption $a(\lambda)$, backscattering $b_b(\lambda)$ and remote sensing reflectance $R_{rs}(\lambda)$, originally developed for the coastal waters of the Southern Baltic Sea, for three selected Pomeranian lakes. Our multi-parameter algorithms are based on the input concentrations of the biogeochemical components measured in the lake waters, i.e., chlorophyll a (*Chl a*), suspended particulate matter (*SPM*), inorganic suspended particulate matter (SPM_{inorg}), the sum of the surface concentrations of accessory pigments (ΣC) and coloured dissolved organic matter with a wavelength of 400 nm ($a_{CDOM}(400)$). $R_{rs}(\lambda)$ and $a(\lambda)$ output values were compared with independent measurements of these parameters conducted in the lake waters at 20 sampling stations. Our algorithm output values of $b_b(\lambda)$ were compared to the values obtained based on the algorithm provided by Ficek, previously developed and validated for Pomeranian lakes, at the same stations. The statistical analyses conducted afterwards showed that the multi-parameter algorithms of $R_{rs}(\lambda)$ and $a(\lambda)$ for the Southern Baltic Sea are sufficient to be used for the stations investigated in the aforementioned three lakes. Specifically, the correlations between the $b_b(\lambda)$ values obtained based on the Ficek algorithm and the $b_b(\lambda)$ values obtained using our multi-parameter algorithm reveal a statistical error rate of less than 20%.

Keywords: bio-optical algorithm; optically complex waters; lakes; inland waters; remote sensing reflectance; absorption coefficient; backscattering coefficient; suspended particulate matter

check for updates

Citation: Lednicka, B.; Kubacka, M.; Freda, W.; Haule, K.; Ficek, D.; Sokólski, M. Multi-Parameter Algorithms of Remote Sensing Reflectance, Absorption and Backscattering for Coastal Waters of the Southern Baltic Sea Applied to Pomeranian Lakes. *Water* **2023**, *15*, 2843. https://doi.org/10.3390/w15152843

Academic Editors: Michael Twiss and Aldona Dobrzycka-Krahel

Received: 12 June 2023
Revised: 27 July 2023
Accepted: 4 August 2023
Published: 6 August 2023

1. Introduction

In terms of optics, the division of water bodies was introduced in 1977 by Morel and Prieur [1], who identified "Case 1 waters" and "Case 2 waters". In subsequent years, Gordon and Morel refined this classification [2,3], and thus, Case 1 waters [4] were found to constitute nearly 98% of the volume of all ocean waters. Case 1 waters (mostly open ocean waters) are areas where their optical properties are primarily determined by autogenous (locally produced) components of seawater, mainly phytoplankton and suspended particulate matter (*SPM*). Moreover, the concentrations of these components (phytoplankton, organic detritus and organic suspended particulate matter (SPM_{org})) correlate statistically with the concentration of chlorophyll a (*Chl a*) [5].

Whenever the optical properties of water indicate the presence of substances of allogeneic origin (coming from the outside, e.g., from river waters in the form of suspended particles, sediments, coloured dissolved organic matter (*CDOM*) and river phytoplankton, as well as from the precipitation of atmospheric dust of urban, industrial or volcanic origin, or coming from dredged material dumping or pollutants, etc.), these are classified as Case 2 waters (mostly coastal waters, bays, semi-closed seas and lakes) [6,7]. This type of water includes, among others, the Baltic Sea and Pomeranian lakes [5–9]. Water-quality-related research is especially important in near-shore basins which are under the direct influence of pollution linked to human activities [10,11]. Similarly, monitoring water quality in inland water bodies is of growing importance in the context of the carbon cycle and regional climate change [12,13]. Recently, numerous optics-related research projects have been conducted in lakes [14,15], and successful attempts have been made to monitor key optical parameters from space on a regular basis [16,17].

Understanding the mutual relations between the inherent optical properties (*IOPs*) and the apparent optical properties (*AOPs*) of a water body and changes in the solar light transfer in the sea as a result of the appearance of water admixtures is an important issue in the optics of the sea, especially when developing satellite methods for monitoring marine and lake environments [18–20]. For example, the *Chl a* concentration can be used as a proxy for a lake's trophic state [20]. Moreover, the knowledge of these relationships allows for the estimation of optical values that are more difficult to determine empirically, e.g., the backscattering coefficient (b_b). This parameter plays a significant role in the assessment of the so-called "ocean colour", i.e., the basic optical parameter calculated as a weighted ratio of remote sensing reflectance (R_{rs}) values for different wavelengths, measured by sensors placed on satellites. The value of R_{rs} is proportional to the value of b_b [21]. Therefore, measurements provided on this scale and the development of semi-empirical models to understand the biogeochemical background will greatly benefit from the remote monitoring of Case 2 waters, especially lakes.

Over the past decades, many bio-optical algorithms for Case 2 waters have been developed. They are usually based on equations describing the physical relationships between IOPs and AOPs as well as statistical correlations between IOPs and the concentrations of biogeochemical components of seawater [22–27].

In 2013, Ficek showed similarities between the eutrophic waters of the Baltic Sea and the Pomeranian, Estonian and Scandinavian lakes in terms of optical properties and optically significant water components [14]. On the basis of relevant research and analyses, he developed a semi-empirical model of light absorption by *SPM* in Pomeranian lakes, which allowed for determining the absorption spectra for phytoplankton and particles other than algae, taking into account the known concentrations of *Chl a* or *SPM*. In addition, Ficek derived a spectral model for the waters of Pomeranian lakes, which allows for calculating the value of the backscattering coefficient ($b_b(\lambda)$) for any wavelength in the VIS range based on the known concentrations of *SPM* or *Chl a*. Ficek also showed that some semi-empirical models and algorithms developed for waters in other regions can be adapted to Pomeranian lakes. He stated that these algorithms should be modified by determining and introducing into the equations other values of the coefficients that would be characteristic of Pomeranian lakes. Since then, more publications have appeared that address the possibility of using marine algorithms for lake waters, e.g., [16,28,29]. In 2016, Meler et al. [28] presented models for estimating the absorptive properties of coloured dissolved organic matter (*CDOM*) for the Baltic Sea and Pomeranian lakes. They developed two empirical mathematical models that enabled them to design the absorption coefficients of coloured dissolved organic matter (a_{CDOM}) dynamics in natural waters and reconstruct the complete a_{CDOM} spectrum in the UV and visible spectral domains. The input variable in the first model was *Chl a*, and in the second one, it was the surface absorption coefficient of CDOM at 400 nm ($a_{CDOM}(400)$). The comparison of these approximations with other models of light absorption by CDOM demonstrated that their parameterisations were superior for estimating CDOM absorption in the optically complex waters of the Baltic Sea and Pomeranian lakes [28].

The utility and various applications of algorithms have been widely presented in the existing literature. Some of the articles address algorithms specifically developed and implemented to obtain coefficients that serve as an indicator of water quality, and some are used to study lake ecosystems [30–33]. Other algorithms help in exploring the relationship between lakes and rivers. For example, in 2021, Jiang et al. proposed an algorithm to monitor rivers' backflow into lakes using satellite images of Lake Poyang (the largest freshwater lake in China) [34]. The proposed solution allowed for independence from hydrological stations, which up until that point had been needed for lake monitoring.

The Baltic Sea is characterised by a low salinity compared to the waters of the oceans and most seas, and thus it is referred to as a brackish sea. This is mainly due to the predominance of the inflow of river waters and rainwater over the inflow of salty waters from the Kattegat. Our multi-parameter algorithms of $a(\lambda_i)$, $b_b(\lambda_i)$ and $R_{rs}(\lambda_i)$ developed for the coastal waters of the southern Baltic Sea [22] were based on in situ optical measurements carried out in the coastal zone (see Figure 1), where freshwater inflows occurred. In some of the studied sites, the salinity was as low as 4 PSU. On the other hand, the salinity of Łebsko Lake may even reach 3 PSU. Therefore, we decided to investigate whether the bio-optical algorithms developed for the coastal waters of the Baltic Sea can be applied to Pomeranian lakes. Based on this premise, the authors decided to investigate the possibility of using the multi-parameter algorithms of $a(\lambda_i)$, $b_b(\lambda_i)$ and $R_{rs}(\lambda_i)$, developed for the coastal waters of the southern Baltic Sea [22], for three selected Pomeranian lakes (Łebsko, Chotkowskie and Obłęskie).

Figure 1. Location of the study area and sampling stations.

2. Materials and Methods

2.1. Multi-Parameter Algorithms of $R_{rs}(\lambda_i)$, $a(\lambda_i)$ and $b_b(\lambda_i)$

For the analysis, the authors used five-parameter algorithms of $R_{rs}(\lambda_i)$ and $a(\lambda_i)$, and a two-parameter algorithm of $b_b(\lambda_i)$ developed for the coastal waters of the southern Baltic Sea and described in [22], where λ_i = 420, 488, 555 and 620 nm. The $R_{rs}(\lambda_i)$ model is a mathematical description of the relationships between the concentrations and properties of natural water components (*Chl a*, *SPM*, SPM_{inorg}, ΣC and $a_{CDOM}(400)$) and the following optical properties: the absorption coefficient of phytoplankton $a_{ph}(\lambda_i)$, the absorption coefficient of non-algal particles $a_d(\lambda_i)$, the absorption coefficient of CDOM $a_{CDOM}(\lambda_i)$ and the backscattering coefficient $b_b(\lambda_i)$. The model was based on the following equation [21]:

$$R_{rs}(\lambda_i) = \left[\frac{f}{Q}\right]_{\lambda_i} \frac{b_b(\lambda_i)}{a(\lambda_i) + b_b(\lambda_i)} \tag{1}$$

In the above equation, the backscattering coefficient $b_b(\lambda_i)$ was estimated as follows [5]:

$$b_b(\lambda_i) = b_{bp}(\lambda_i) + b_{bw}(\lambda_i), \tag{2}$$

where $b_{bp}(\lambda_i)$ is the backscattering coefficient of particles and $b_{bw}(\lambda_i)$ is the backscattering coefficient of water molecules given by Morel [35]. The absorption coefficient $a(\lambda_i)$ was calculated as the sum of the following [5]:

$$a(\lambda_i) = a_{CDOM}(\lambda_i) + a_{ph}(\lambda_i) + a_d(\lambda_i) + a_w(\lambda_i), \tag{3}$$

where $a_w(\lambda_i)$ is the absorption coefficient of seawater molecules [36].

The values of $[f/Q]_{\lambda i}$ parameter were calculated for the chosen areas of the southern Baltic Sea based on a large dataset of measurements of $L_u(\lambda_i)$, $E_d(\lambda_i)$, $b_b(\lambda_i)$ and $a(\lambda_i)$ (Table 1). Having assumed the above, it was possible to determine $R_{rs}(\lambda_i)$ for four wavelengths in the visible light range using the knowledge of the concentration of admixture components in the coastal waters of the southern Baltic Sea based on Equations (4)–(7) [22].

$$b_{bp}(\lambda_i)_{cal} = \mathrm{B}_1(\lambda_i) SPM^{\mathrm{B}_2(\lambda_i)} e^{\mathrm{B}_3(\lambda_i)\frac{SPM_{inorg}}{SPM}} \tag{4}$$

$$a_{CDOM}(\lambda_i)_{cal} = 10^{[\mathrm{O}_1(\lambda_i)(a_{CDOM}(400))^2 + \mathrm{O}_2(\lambda_i) a_{CDOM}(400) - \mathrm{O}_3(\lambda_i)]} \tag{5}$$

$$a_d(\lambda_i)_{cal} = \mathrm{D}_1(\lambda_i) SPM^{\mathrm{D}_2(\lambda_i)} e^{\mathrm{D}_3(\lambda_i)\frac{SPM_{inorg}}{SPM}} \tag{6}$$

$$a_{ph}(\lambda_i)_{cal} = \mathrm{P}_1(\lambda_i) Chl\ a^{\mathrm{P}_2(\lambda_i)} e^{\mathrm{P}_3(\lambda_i)\frac{\Sigma \mathrm{C}}{Chl\ a}} \tag{7}$$

These multi-parameter algorithms were further used to calculate $R_{rs}(\lambda_i)$, $a(\lambda_i)$ and $b_b(\lambda_i)$ for the three chosen lakes. The first stage was to examine the possibility of using the five-parameter total absorption algorithm to calculate $a(\lambda_i)$ for the selected lakes. For this purpose, we used Equations (3) and (5)–(7) as well as relevant constants (Table 1). Next, based on Equations (2) and (4) and Table 1, $b_b(\lambda_i)$ was calculated. The last step was to calculate $R_{rs}(\lambda_i)$ based on Equation (1) and previously determined $a(\lambda_i)$ and $b_b(\lambda_i)$. The values of $[f/Q]_{\lambda i}$ parameters used for calculations of $R_{rs}(\lambda_i)$ of lake waters, presented in Table 1, come from [22].

Table 1. The constants of the five-parameter model of $a(\lambda_i)$, the two-parameter model of $b_b(\lambda_i)$ and the five-parameter model of $R_{rs}(\lambda_i)$ (Equations (4)–(7)).

λ_i	**420**	**488**	**555**	**620**
B_1	0.009	0.006	0.005	0.004
B_2	0.911	0.891	0.935	0.881
B_3	0.337	0.827	0.977	1.230
O_1	0.077	0.624	1.037	1.488
O_2	1.006	1.077	1.072	1.136
O_3	0.132	0.485	0.689	0.794
D_1	0.057	0.035	0.022	0.015
D_2	0.807	0.762	0.646	0.592
D_3	0.750	0.903	1.157	1.542
P_1	0.041	0.022	0.011	0.007
P_2	0.827	0.820	0.815	0.926
P_3	0.493	0.824	0.257	0.261
b_{bw}	0.0023	0.0012	0.0007	0.0004
a_w	0.0045	0.0147	0.0596	0.2755
f/Q	0.07	0.10	0.12	0.13

2.2. Study Area

The multi-parameter marine algorithms were previously developed on the basis of measurements carried out in the area of the southern Baltic Sea, i.e., the Gulf of Gdańsk, Szczecin Lagoon and the Southern Baltic Sea coastal zone (Figure 1). In order to examine the possibility of using these algorithms in lake waters, we used empirical materials collected during several field trips to the lakes of the Pomeranian Lake District: Łebsko, Chotkowskie and Obłęskie (Figure 1). Łebsko Lake is the third largest lake in Poland, with an area of 71 km^2 and a maximum depth of 6.3 m. It is a coastal lake separated from the sea by a sandy spit. The basin is a remnant of the former sea bay, the Łeba River is its tributary and it is also connected by canals with Gardno and Sarbsko Lakes [37]. Chotkowskie Lake is a glacial lake with a total area of 0.56 km^2 and a maximum depth of 10.3 m. The third of the analysed lakes, Obłęskie Lake, is a flow-through lake, connected by a small stream with the Wieprza River basin. The maximum depth of the lake is 8.9 m, and it covers an area of 0.62 km^2 [14]. These lakes represent three optical lake types in Northern Poland according to [38].

2.3. Data Acquisition and Processing

The acquisition and processing of the data used to develop marine multi-parameter algorithms are described in [22]. In situ R_{rs} spectra in lakes were measured with the HyperOCR (Satlantic Inc., Halifax, NS, Canada) instrument and processed according to the standard procedure described in [22]. At the same sampling stations, separate water samples were also collected for laboratory measurements of the following parameters: the concentration of chlorophyll *Chl a* (absorption spectrum of the pigment ethanol extract) [39] and the mass concentration of the total suspension *SPM* and its inorganic fraction SPM_{inorg} (standard gravimetric method) [40]. The composition of accessory pigments ΣC (the sum of chlorophyll b, chlorophyll c, and photosynthetic and photoprotective pigments) was determined using HPLC method (high-performance liquid chromatography) [41]. The absorption coefficient of CDOM at 400 nm ($a_{CDOM}(400)$) was obtained using spectrophotometric analysis followed by two-step filtration [42].

All parameters were tested in a manner resembling the test methods used previously for the Southern Baltic Sea. Finally, the analysed materials from the three Pomeranian lakes included 20 sets of measurement data for the surface water layer (*Chl a*, ΣC, *SPM*, SPM_{inorg}, $a_{CDOM}(400)$, $L_u(0^-)$ and $E_d(0^-)$).

To analyse the data, we used arithmetic and logarithmic statistical methods. Lake waters are areas of high diversity in terms of water physics and chemistry. The concentrations of biogeochemical constituents for the three lakes varied up to three orders of magnitude. Therefore, we applied logarithmic statistics in addition to arithmetic statistics, for more accurate evaluation of the relationship between the measured values and the calculated ones.

3. Results

3.1. Remote Sensing Reflectance R_{rs} Estimated for the Lakes of the Pomeranian Lake District

The empirical materials collected during the spring and summer months (from April to July) from the Łebsko, Chotkowskie and Obłęskie Lakes are characterised by high concentrations of *Chl a* (from 8.6 mg·m^{-3} up to 81.6 mg·m^{-3}), SPM_{inorg} (from 1.2 g·m^{-3} to 21.1 g·m^{-3}) and SPM_{org} (from 2.6 g·m^{-3} to 51.3 g·m^{-3}). The data for the Southern Baltic Sea waters that were used to develop the algorithms of $R_{rs}(\lambda_i)$, $a(\lambda_i)$ and $b_b(\lambda_i)$ were collected both in the spring and during the autumn–winter months and are characterised by significantly lower concentrations of *Chl a*, SPM_{inorg} and SPM_{org} (the average concentration of *Chl a* was 9.8 mg·m^{-3}, the average concentration of SPM_{inorg} was 1.1 g·m^{-3} and the average concentration of SPM_{org} was 3.2 g·m^{-3}). All the measured R_{rs} spectra for each studied lake are shown in Figure 2 below. There are differences both the spectral shape and range of R_{rs} values for each water basin. Łebsko Lake usually had high R_{rs} values and a high peak at 705 nm, which is characteristic for CDOM-rich eutrophic waters. In the case of Chotkowskie Lake, the R_{rs} values were much lower with more diverse shapes, while Obłęskie Lake had the widest range of recorded R_{rs} values and the highest peak in the central part of the visible spectrum.

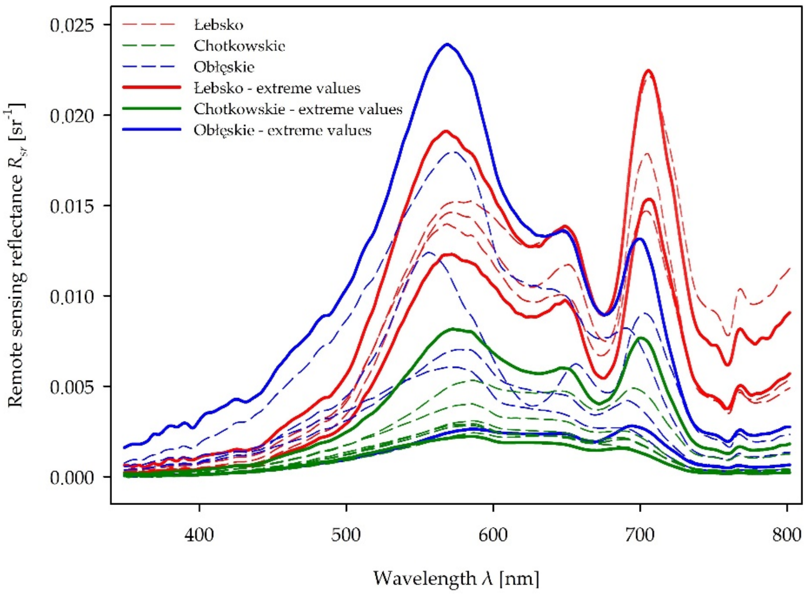

Figure 2. Spectra of the remote sensing reflectance measured with HyperOCR (Satlantic Inc.) in three Pomeranian lakes: Łebsko (red line), Chotkowskie (green line) and Obłęskie (blue line).

Figure 3 below presents the graphs of the R_{rs} values determined using the HyperOCR meter $R_{rs}(\lambda_i)_m$, in relation to the values calculated on the basis of the five-parameter model of R_{rs} for the Southern Baltic Sea $R_{rs}(\lambda_i)_{cal}$ and the probability density distributions of the calculated R_{rs} to the measured R_{rs} ratio for four wavelengths.

The obtained estimation errors of $R_{rs}(\lambda_i)$ are shown in Table 2. Comparing the values of $R_{rs}(\lambda_i)_m$ measured in lakes with the HyperOCR radiometer and those calculated on the basis of the five-parameter $R_{rs}(\lambda_i)_{cal}$ for the Southern Baltic coastal waters, it is clearly visible that the $R_{rs}(\lambda_i)_{cal}$ coefficients calculated using the model take higher values than the $R_{rs}(\lambda_i)_m$ obtained by way of measurements, especially for the wavelengths of 488 nm and 555 nm (see the histograms in Figure 3). Therefore, the systematic errors have positive values (Table 2).

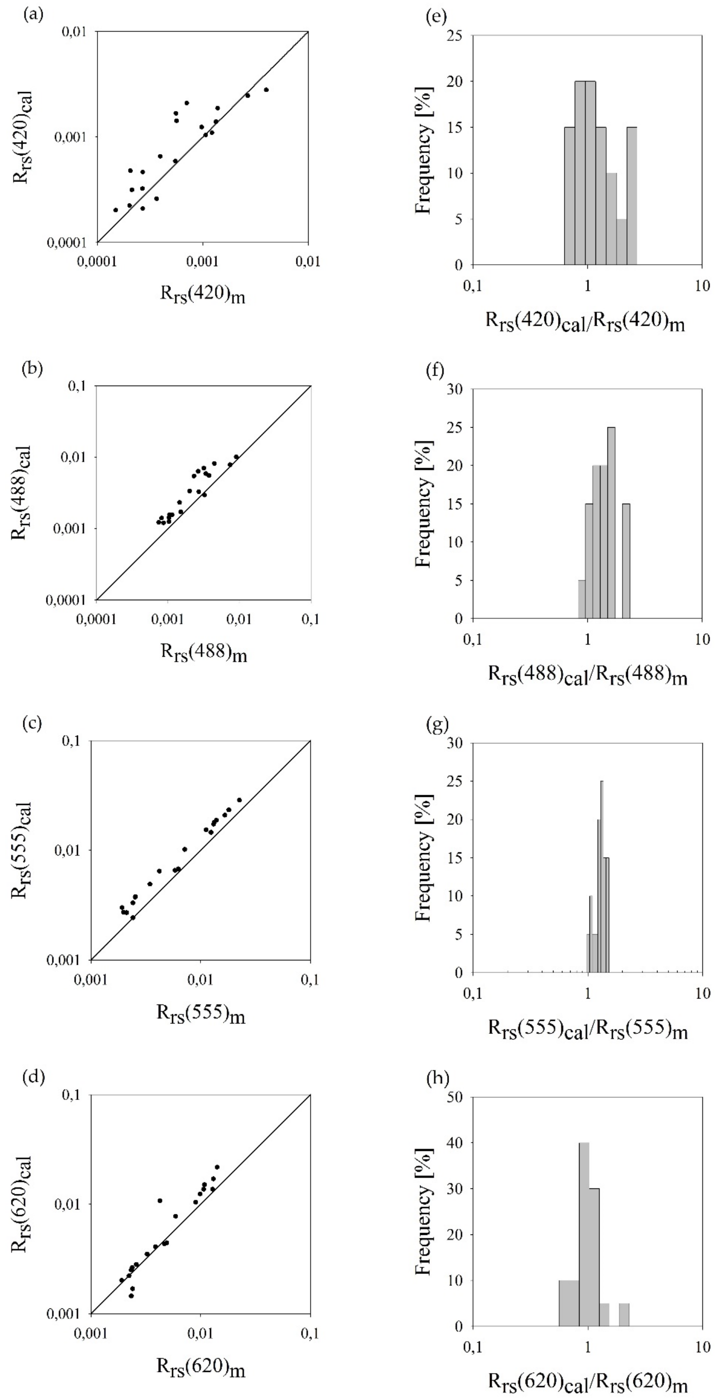

Figure 3. (**a**–**d**) Correlation plots of the calculated $R_{rs}(\lambda_i)_{cal}$ versus the measured $R_{rs}(\lambda_i)_m$ for the following wavelengths: λ_i = 420 nm, 488 nm, 555 nm and 620 nm for three lakes: Łebsko, Chotkowskie and Obłęskie. The solid line represents the linear function $R_{rs}(\lambda_i)_m = R_{rs}(\lambda_i)_{cal}$. (**e**–**h**) Corresponding probability density distributions of the ratio of the calculated $R_{rs}(\lambda_i)_{cal}$ to the measured $R_{rs}(\lambda_i)_m$.

The strongest correlation (R^2 > 0.9) was achieved for 555 nm and 620 nm and the weakest (R^2 = 0.53) for 420 nm. The highest consistency between the measured and the calculated R_{rs} was obtained for 620 nm, which is the minimum for remote sensing reflectance corresponding to the maximum for water absorption. On the other hand, the most linear correlation obtained for 550 nm corresponds to the maximum for R_{rs} which is the minimum for absorption. The statistical logarithmic errors vary from −36.00% to +56.25%.

Table 2. Definitions and values of relative errors of the $R_{rs}(\lambda_i)$ coefficients for three lakes in the Pomeranian Lake District (Łebsko, Chotkowskie and Obłęskie Lakes) (for the wavelengths: 420, 488, 555 and 620 nm), calculated on the basis of the five-parameter R_{rs} for chosen stations in the Southern Baltic Sea [22].

Arithmetic Statistic of $R_{rs}(\lambda)$ [%]		$R_{rs}(420)$	$R_{rs}(488)$	$R_{rs}(555)$	$R_{rs}(620)$
Relative mean error $\langle\varepsilon\rangle = \frac{1}{N}\sum_i \varepsilon_i,$		45.41	54.96	32.74	17.42
RMSE—root mean square error of ε $\sigma_\varepsilon = \sqrt{\frac{1}{N}\left(\sum_i (\varepsilon_i - \langle\varepsilon\rangle)^2\right)}$		71.34	41.84	14.77	38.72
Logarithmic Statistic of $R_{rs}(\lambda)$ [%]		$R_{rs}(420)$	$R_{rs}(488)$	$R_{rs}(555)$	$R_{rs}(620)$
Mean logarithmic error $\langle\varepsilon\rangle_g = 10^{g_i} - 1$		31.58	49.86	31.92	12.61
Standard error factor $x = 10^{\sigma_{log}},$		1.56	1.30	1.12	1.33
Statistical	$\sigma_+ = x - 1$	56.25	30.27	12.25	33.21
logarithmic errors	$\sigma_- = x^{-1} - 1$	−36.00	−23.24	−10.91	−24.93

where:
$X_{i,m}$—measured values of $R_{rs}(\lambda_i)$; $X_{i,cal}$—estimated values of $R_{rs}(\lambda_i)$,
$\varepsilon_i = \left(\frac{X_{i,cal} - X_{i,m}}{X_{i,m}}\right)$, $g_i = log\left(\frac{X_{i,cal}}{X_{i,m}}\right)$, $\sigma_{log} = \sqrt{\frac{1}{N}\left(\sum_i (g_i - \langle g\rangle)^2\right)}$, $\langle g\rangle = \frac{1}{N}\sum_i g_i$

The values of statistical errors (Table 2) affecting the R_{rs} calculated for lakes on the basis of the five-parameter R_{rs} model exceed 50% only for a wavelength of 420 nm. For other wavelengths, the statistical error rate is much lower, and for 620 nm, it is a small percentage. Moreover, the greatest differences in the values of $R_{rs}(\lambda_i)_{cal}$ and $R_{rs}(\lambda_i)_m$ are observed for a wavelength of 420 nm, for which the standard error factor has the highest value x = 1.56 (Table 2, Figure 3). This corresponds to the spectral region of significant influence of $a_{CDOM}(\lambda_i)$ on $a(\lambda_i)$.

3.2. Absorption Coefficients Estimated for the Lakes of the Pomeranian Lake District

The total absorption values measured in the tested Pomeranian lakes at the four tested wavelengths are presented in Figure 4. The highest values were obtained at 420 nm in the region of strong CDOM absorption. Samples no. 1–5 characterised by the highest absorption values and range were collected in Łebsko Lake. Samples no. 6–13 were collected in Chotkowskie Lake and samples no. 14–20 in Obłęskie Lake.

Figure 5 below presents the comparison of the measured and modelled absorption coefficients for lake waters. The values of absorption coefficients measured in lakes $a(\lambda_i)_m$ for the three wavelengths (420, 488 and 555 nm) in most cases are higher than the values of the absorption coefficients calculated on the basis of the five-parameter model $a(\lambda_i)_{cal}$. Only for the wavelength of 620 nm, the values of the absorption coefficients obtained on the basis of the calculations are mostly higher than the measured ones.

The strongest correlation (R^2 > 0.9) was obtained for 420 nm. The statistical error rates of the light absorption coefficients that were calculated using the five-parameter model of absorption range from 10% to 70% (Table 3). This indicates that the diversity of the chemical composition of the suspended and dissolved matter greatly influences the optical absorption capacity. Relatively small values of the standard error factors presented in Table 3 (except for the 620 nm wavelength, where x = 1.69) show good agreement between the results obtained with the use of the five-parameter absorption model and the measurements in the lake waters. The statistical logarithmic errors range from −40.92% to +69.26%.

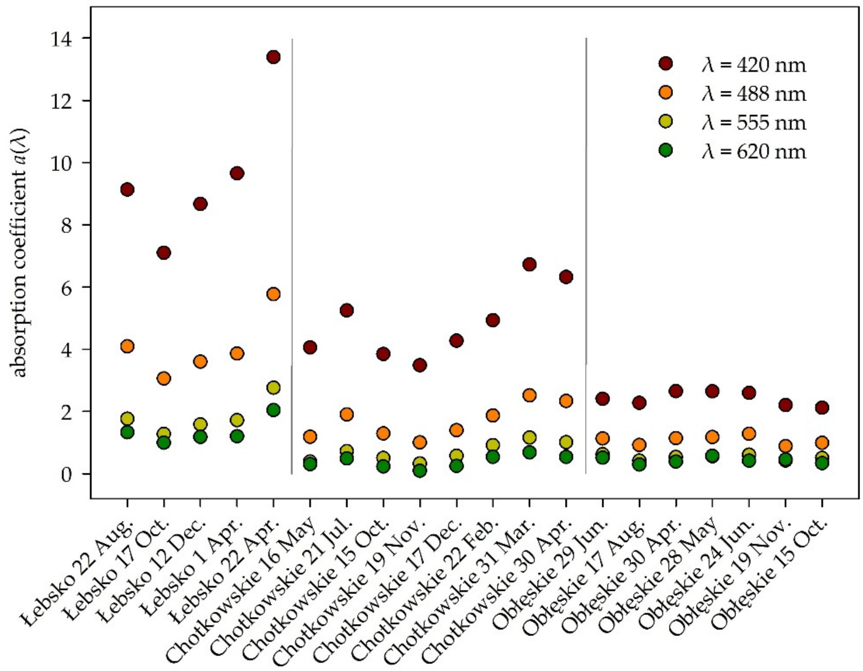

Figure 4. Values of the total absorption coefficient measured at four wavelengths (420 nm, 488 nm, 555 nm and 620 nm) in three Pomeranian lakes: Łebsko, Chotkowskie and Obłęskie during twenty measurement campaigns.

Table 3. Relative errors in the total absorption coefficients $a(\lambda)$ for the wavelengths: 420, 488, 555 and 620 nm for three lakes in the Pomeranian Lake District (Łebsko, Chotkowskie and Obłęskie Lakes), calculated on the basis of the total absorption model for selected waters of the Southern Baltic Sea [22]. The measurements were completed using 20 sets of data for the surface layer.

Arithmetic Statistic of $a(\lambda)$ [%]		**$a(420)$**	**$a(488)$**	**$a(555)$**	**$a(620)$**
Relative mean error $\langle\varepsilon\rangle = \frac{1}{N}\sum_i \varepsilon_i$,		−7.49	−10.35	−3.66	65.97
RMSE—root mean square error of ε $\sigma_\varepsilon = \sqrt{\frac{1}{N}\left(\sum_i(\varepsilon_i - \langle\varepsilon\rangle)^2\right)}$		10.65	23.92	35.63	11.07
Logarithmic Statistic of $a(\lambda)$ [%]		**$a(420)$**	**$a(488)$**	**$a(555)$**	**$a(620)$**
Mean logarithmic error $\langle\varepsilon\rangle_g = 10^{g_i} - 1$		−8.05	−13.14	−10.08	42.82
Standard error factor $x = 10^{\sigma_{log}}$,		1.12	1.29	1.48	1.69
Statistical logarithmic errors	$\sigma_+ = x - 1$,	29.19	47.51	69.26	33.21
	$\sigma_- = x^{-1} - 1$,	−22.59	−32.21	−40.92	−24.93

where:
$X_{i,m}$—measured values of $a(\lambda_i)$; $X_{i,cal}$—estimated values of $a(\lambda_i)$,
$\varepsilon_i = \left(\frac{X_{i,cal} - X_{i,m}}{X_{i,m}}\right)$, $g_i = log\left(\frac{X_{i,cal}}{X_{i,m}}\right)$, $\sigma_{log} = \sqrt{\frac{1}{N}\left(\sum_i (g_i - \langle g\rangle)^2\right)}$, $\langle g\rangle = \frac{1}{N}\sum_i g_i$

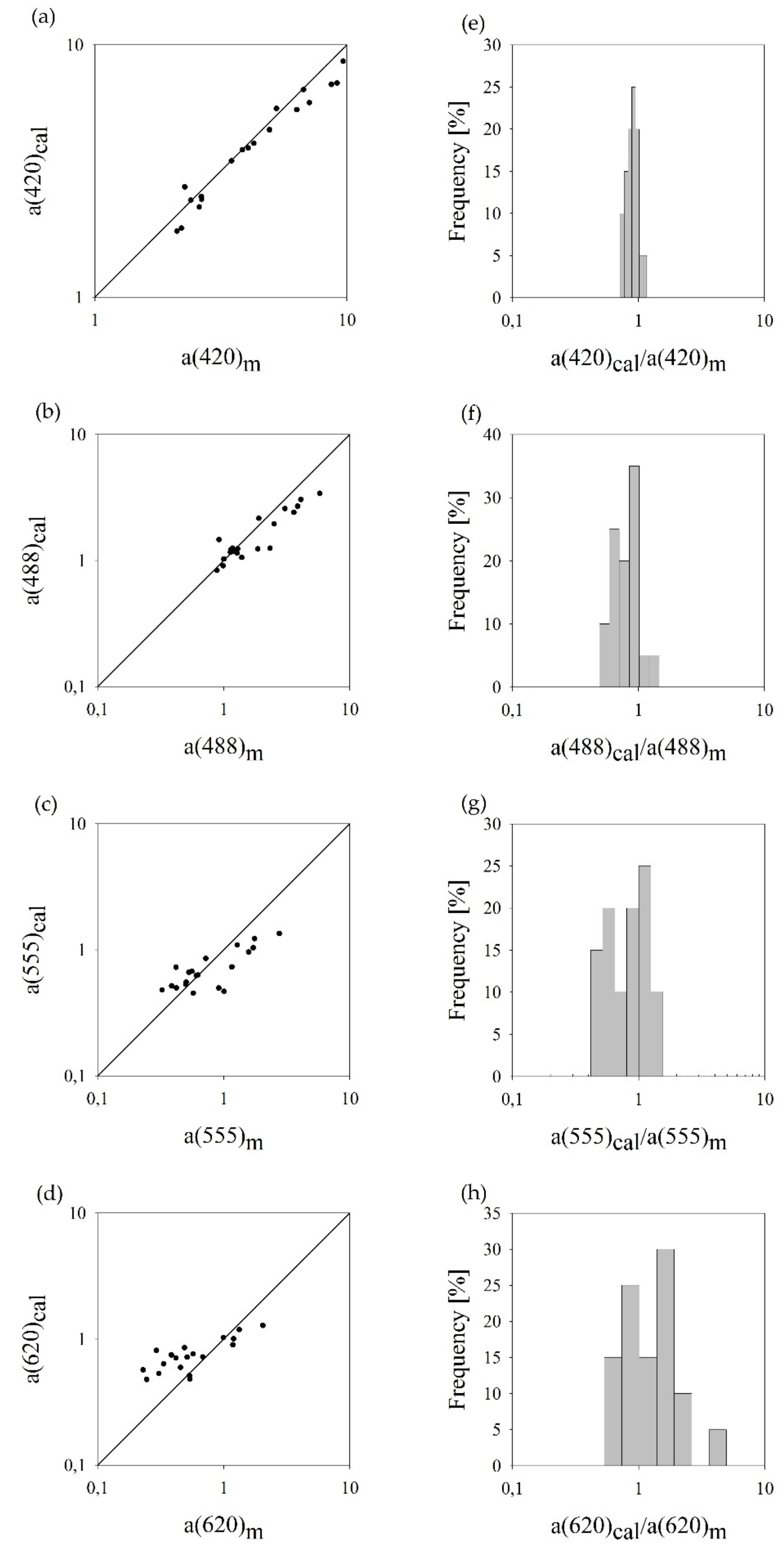

Figure 5. (**a**–**d**) Correlation plots of the calculated $a(\lambda_i)_{cal}$ versus the measured $a(\lambda_i)_m$ for the wavelengths a_i = 420 nm, 488 nm, 555 nm and 620 nm for three lakes: Łebsko, Chotkowskie and Obłęskie. The solid line represents the linear function ($a(\lambda_i)_m = a(\lambda_i)_{cal}$). (**e**–**h**) Corresponding probability density distributions of the ratio of the calculated $a(\lambda_i)_{cal}$ to the measured $a(\lambda_i)_m$.

3.3. Backscatttering Coefficient Comparison between Two Algorithms

In the case of the backscattering coefficient $b_b(\lambda_i)$, we applied a semi-empirical method based on the regression equation between $b_b(\lambda_i)$ and SPM for Pomeranian lakes in 2009–2010 developed by Ficek [12]. None of the wavelengths used in the multi-parameter model coincided with the wavelength used by Ficek, i.e., 532 nm. Therefore, the b_b at 532 nm was estimated by linearly approximating the data from the two nearby wavelengths: 488 nm and 550 nm. The difference in the values of $b_b(532)$ calculated according to Ficek's algorithm [14] and those calculated on the basis of Lednicka and Kubacka [22] is small (Figure 6). The $b_b(532)$ calculated according to Ficek [14] clearly is slightly higher than the values calculated using the algorithm by Lednicka and Kubacka [22]. This tendency can be noted for all twenty measurements taken with regard to the lakes of the Pomeranian Lake District (see Figure 6).

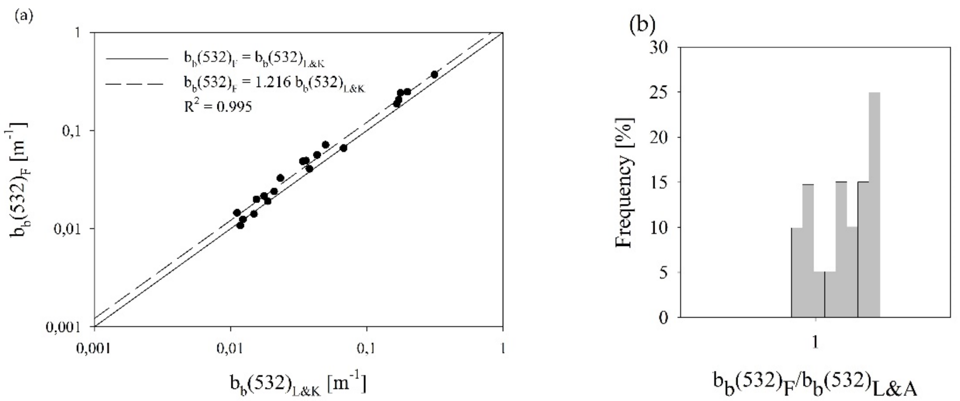

Figure 6. (**a**) Comparison of the $b_b(532)_F$ based on Ficek's algorithm and the calculated $b_b(532)_{L\&K}$ based on Lednicka and Kubacka for three lakes: Łebsko, Chotkowskie and Obłęskie. (**b**) Corresponding probability density distribution of the $b_b(532)_F$ to $b_b(532)_{L\&}$ ratio.

The relative differences between $b_b(532)$ for the three lakes of the Pomeranian Lake District (Łebsko, Chotkowskie and Obłęskie), calculated on the basis of the b_b model for the Southern Baltic Sea [22] and based on Ficek's algorithm [12], are as follows:

- A relative mean error $\langle\varepsilon\rangle$ of 19.89%;
- A root mean square error σ_ε of 16.76%;
- A mean logarithmic error $\langle\varepsilon\rangle_g$ of 18.74%;
- A standard error factor x of 1.15;
- A statistical logarithmic error σ_+ of 15.45% and σ_- of 13.38%.

A high correlation between $b_b(532)_F$ and $b_b(532)_{L\&K}$ is confirmed by the rate of statistical errors that affect the b_b values, which range from 13% to 17%.

4. Discussion

4.1. Performance of the Rrs Model in Lakes

The remote sensing of lakes is probably just as important (because of the need to control water quality and climate change) as it is challenging (because of the high spatial and temporal variability in lake water components) [9,16]. Similarly to that of near-shore waters and river estuaries, it requires a strictly local approach, and there are many advantages of applying existing marine bio-optical models for inland waters [16]. The presented study aims to analyse the applicability of a set of multi-parameter algorithms for the Southern Baltic Sea as described in [22] to Pomeranian lakes.

The performance of multi-parameter models was evaluated using several statistical measures. The most commonly used one is the root mean squared error (RMSE), which shows differences between values measured in situ and values predicted by a model. The highest RMSE for the remote sensing reflectance was obtained at 420 nm, where the range of the measured values was the greatest. This is also the spectral region with the highest absorption by CDOM of all tested wavelengths [43] and the region with the lowest R_{rs} signal. The studied Pomeranian lakes are CDOM-dominated waters, and high CDOM absorption reduces the R_{rs}. The five-parameter R_{rs} model worked less efficiently for low R_{rs} values (RMSEs of over 70% at 420 nm) and was the most efficient for high R_{rs} values (RMSEs of less than 15% at 555 nm). Ficek et al. [38] divided Pomeranian lakes into three groups according to the shape of the remote sensing reflectance spectra, and this study covers a representative of each group: waters with high CDOM (Chotkowskie Lake), waters with low CDOM but high *Chl a* (Obłęskie Lake) and waters with moderate concentrations of all optically significant constituents (Łebsko Lake)—see Figure 1 in [38]. The structure of the tested multi-parameter models was based on a set of constants calculated on the basis of a large dataset of ship cruises spanning several years. The f/Q constant depends on the irradiance conditions and geometry between the sun and the sensor's position and is usually assumed to be wavelength independent, although by definition, it depends on λ [44] and is considered seasonally dependent [45]. In our five-parameter R_{rs} model, the wavelength-dependent f/Q was applied as the most accurate for the Southern Baltic Sea. Although the 20 measurements taken in the Pomeranian lakes are not enough to draw substantial conclusions, we believe that the performance of our multi-parameter model is encouraging enough for such tests to be continued in inland waters. After gathering a larger dataset covering inland waters, it will be possible to calculate specific f/Q factors for these waters and improve the model's accuracy.

4.2. Performance of the Absorption Model in Lakes

Water absorption properties result from all optically significant components in a given body of water and strongly depend on their concentrations and chemical composition. Among organic particles, there are over twenty chemical types differing in terms of absorption properties. For mineral particles, there are at least a dozen types of these minerals with different chemical compositions [46]. In coastal zones, especially in river mouths, $a_{CDOM}(\lambda_i)$ can be very high and determine the entire light absorption spectrum [47]. Figure 5 presents graphs for four wavelengths: 420, 488, 555 and 620 nm, regarding the relative share of a_{CDOM} (λ_i), $a_{ph}(\lambda_i)$ and $a_d(\lambda_i)$ for selected stations in the Southern Baltic Sea and the studied lakes in the Pomeranian Lake District. A significant difference can be observed in the chemical composition of sea and lake waters. The first three graphs show a strong advantage of a_{CDOM} for both the lakes and coastal waters of the Southern Baltic Sea (in the case of the seawater, the average percentage share for these three wavelengths is well above 50%). In the case of the lakes, there is also a large contribution of $a_d(\lambda_i)$, the average percentage of which for all wavelengths is high, and for 555 nm, it is even 37%. In the case of both the lake waters and the Southern Baltic Sea waters at a wavelength of 420 nm, the $a_{CDOM}(\lambda_i)$ has the greatest contribution to the spectrum of the entire absorption, and its average percentage share is 58% for the lakes and 68% for the Baltic coastal waters (the average percentage share of other absorption coefficients for the lakes is $a_{ph}(\lambda_i)$—20% and $a_d(\lambda_i)$—22% and for the selected reservoirs of the Southern Baltic Sea is $a_{ph}(\lambda_i)$—20% and $a_d(\lambda_i)$—12%, respectively). The average percentage share of a_{CDOM} (λ_i), $a_{ph}(\lambda_i)$ and $a_d(\lambda_i)$ in the absorption process for all wavelengths of the analysed waters is shown in Table 4.

The graphs presented in Figure 7 clearly show a significant difference in the share of various absorption components between the lake waters and the Southern Baltic Sea coastal zone. This differentiation is particularly visible for the longwave part of the spectrum. Therefore, the possibility of using the five-parameter model to calculate the $a(\lambda_i)$ coefficient in the selected lakes of the Pomeranian Lake District was tested. A very good agreement was obtained at 420 nm and a relatively good agreement at other wavelengths, which enables model testing to be continued after gathering a larger dataset. The correlation plots in Figure 3 indicate that a shift on the y-axis could provide a better linear correlation between the modelled data and the measured data. However, such a calibration of the model will most probably be seasonally and locally variable and wavelength dependent, which is why it will require a much larger dataset.

Table 4. Average percentage share of *CDOM*, SPM_{org} and SPM_{inorg} in the absorption process.

Lakes	λ = 420 nm	λ = 488 nm	λ = 555 nm	λ = 620 nm
$a_{ph}(\lambda)$ [%]	20	22	19	35
$a_d(\lambda)$ [%]	22	31	37	33
$a_{CDOM}(\lambda)$ [%]	58	47	44	32
Coastal Waters	**λ = 420 nm**	**λ = 488 nm**	**λ = 555 nm**	**λ = 620 nm**
$a_{ph}(\lambda)$ [%]	20	27	18	19
$a_d(\lambda)$ [%]	12	15	17	17
$a_{CDOM}(\lambda)$ [%]	68	58	65	64

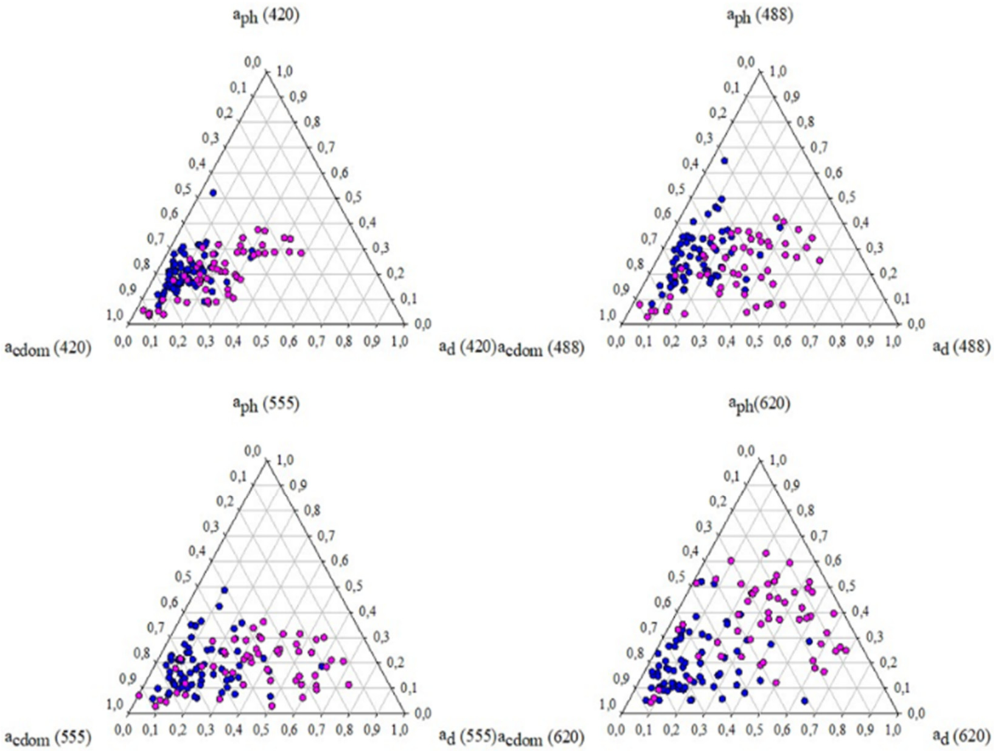

Figure 7. Ternary plots of the relative contribution of CDOM, detritus and phytoplankton pigments to total absorption by non-water constituents for four wavelengths: λ_i = 420 nm, 488 nm, 555 nm and 620 nm in the Southern Baltic Sea (blue dots) and the Pomeranian lakes (pink dots). The higher the relative contribution of a sample, the closer the data point to the corresponding triangle apex.

In 2019, Xue et al. [48] used local data to build a model of IOPs based on satellite $R_{rs}(\lambda)$ data in turbid inland waters. They measured the $R_{rs}(\lambda)$ and absorption coefficients from lakes in the Yangtze River and Huai River basin, China. Their iterative IOP inversion model was developed to retrieve, among others, the total absorption coefficients in turbid lakes. They established that the total absorption coefficients derived from their algorithm have a mean RMSE of 39.45%, ranging from 400 to 720 nm. The RMSEs obtained in our study were, respectively: for 420 nm—10.65%, 488 nm—23.92%, 555 nm—35.63% and 620 nm—11.07%. Here, we again observe better model performance for high absorption values at 420 nm and 620 nm.

4.3. Performance of the Backscattering Model in Lakes

The backscattering coefficient is a fundamental quantity in regulating the optical signal available for remote sensing and is of particularly great importance for optically complex coastal and inland waters [49]. In this study, the correlation between two semi-empirical models was tested: the model developed by Ficek for the Pomeranian lakes and our multi-parameter model developed by Lednicka and Kubacka for the Southern Baltic Sea. Both models were based on different sets of measured data. The backscattering coefficient in the Baltic Sea and optically similar inland waters is strongly spectral dependent [50], and its values can vary by two orders of magnitude [51]. The RMSEs between the two models and the R^2 were almost 17% and 0.995, respectively, which is a very satisfactory result. The data measured in the lake waters were mostly characterised by high concentrations of *Chl a*. However, for low concentrations of *Chl a*, the values of $b_b(\lambda_i)$ measured in the lake waters are very similar to those represented by the turbid coastal waters of the Baltic Sea [14].

5. Conclusions

The study was focused on analysing the possibility of using the multi-parameter algorithms of $a(\lambda_i)$, $b_b(\lambda_i)$ and $R_{rs}(\lambda_i)$, developed for the coastal waters of the Southern Baltic Sea [22], for three Pomeranian lakes. The conducted tests show that the five-parameter model of $R_{rs}(\lambda_i)$ and the five-parameter model of $a(\lambda_i)$ developed for the Southern Baltic Sea can be applied with satisfactory accuracy to the Pomeranian lakes. The RMSE obtained for $R_{rs}(\lambda)$ exceeds 50% only for a wavelength of 420 nm. In the case of $a(\lambda_i)$, the statistical error rates do not exceed 40% for all tested wavelengths.

Moreover, the difference in the $b_b(532)_F$ values obtained on the basis of the Ficek algorithm for the lakes of the Pomeranian Lake District and the $b_b(532)_{L\&K}$ values obtained on the basis of the Lednicka and Kubacka algorithm for the selected areas of the Southern Baltic Sea reveals systematic errors with a rate lower than 20% and statistical errors with a rate below 17%. Although the number of measurements available for testing was relatively small, their range was representative for all optical types occurring in the Pomeranian Lake District. The results obtained encourage us to derive the optical parameters of inland waters using the multi-parameter algorithms developed for the Southern Baltic Sea.

It is commonly known that bio-optical algorithms are designed to associate *AOPs* (especially $R_{rs}(\lambda)$) with *IOPs* and seawater component concentrations. However, the great variety in optically significant constituents of Case 2 waters limits the use of global bio-optical algorithms. This is why we believe that our contribution of the presented results will allow for an expansion of our knowledge about the optical properties of Case 2 waters represented by the lakes of the Pomeranian Lake District and encourage testing, applications and further calibrations of the existing models in inland waters.

Author Contributions: Conceptualisation, B.L.; methodology, B.L.; software, B.L.; validation, B.L. and M.S.; formal analysis, B.L.; investigation, B.L., D.F. and M.S.; resources, B.L. and D.F.; data curation, B.L.; writing—original draft preparation, B.L. and M.K.; writing—review and editing, B.L., M.K., K.H. and W.F.; visualization, B.L., M.K. and W.F.; supervision, B.L.; project administration, B.L.; funding acquisition, B.L. and M.K. All authors have read and agreed to the published version of the manuscript.

Funding: This paper was prepared as a part of project N N306 036836 financed by the Polish Ministry of Science and Higher Education in the years 2009–2014 and also as a part of the SatBałtyk project funded by the European Union through European Regional Development Fund (No. POIG.01.01.02-22-011/09, 'The Satellite Monitoring of the Baltic Sea Environment').

Data Availability Statement: The data that support the findings of this study are available from the corresponding author upon justified request.

Acknowledgments: The authors would like to thank their colleagues from IOPAN: Justyna Meler, Joanna Stoń-Egiert, Agnieszka Zdun, Sławomir Sagan, Mirosława Ostrowska, Sławomir Woźniak, Piotr Kowalczuk and Mirosław Darecki for their help with the field and laboratory measurements.

Conflicts of Interest: The authors declare no conflict of interest.

References

1. Morel, A.; Prieur, L. Analysis of variations in ocean color. *Limnol. Oceanogr.* **1977**, *22*, 709–722. [CrossRef]
2. Gordon, H.R.; Morel, A. *Remote Assessment of Ocean Color for Interpretation of Satellite Visible Imagery, A Review*; Springer: New York, NY, USA, 1983; p. 114.
3. Morel, A. Optical modeling of the upper ocean in relation to its biogenous matter content (Case I waters). *J. Geophys. Res.* **1988**, *93*, 10749–10768. [CrossRef]
4. Mobley, C.D. *Light and Water: Radiative Transfer in Natural Waters*; Academic Press: Cambridge, MA, USA, 1994.
5. Dera, J. *Marine Physics*; PWN: Warszawa, Poland, 2003; pp. 1–514.
6. Haule, K.; Toczek, H.; Borzycka, K.; Darecki, M. Influence of Dispersed Oil on the Remote Sensing Reflectance—Field Experiment in the Baltic Sea. *Sensors* **2021**, *21*, 5733. [CrossRef] [PubMed]
7. Lednicka, B.; Kubacka, M.; Freda, W.; Haule, K.; Dembska, G.; Galer-Tatarowicz, K.; Pazikowska-Sapota, G. Water Turbidity and Suspended Particulate Matter Concentration at Dredged Material Dumping Sites in the Southern Baltic. *Sensors* **2022**, *22*, 8049. [CrossRef]
8. Kaczmarek, S.; Woźniak, B. The application of the optical classification of waters in the Baltic Sea (Case 2 waters). *Oceanologia* **1995**, *37*, 285–297.
9. Haule, K.; Freda, W. Remote Sensing of Dispersed Oil Pollution in the Ocean—The Role of Chlorophyll Concentration. *Sensors* **2021**, *21*, 3387. [CrossRef]
10. Boniewicz-Szmyt, K.; Grzegorczyk, M.; Pogorzelski, S.; Rochowski, P. Photosynthetic signatures of microbial colonies covering submerged hard surfaces as novel trophic status indicators: Baltic Sea studies. *Oceanologia* **2023**, *65*, 194–201. [CrossRef]
11. Baszanowska, E.; Otremba, Z. Detection of Oil in Seawater Based on the Fluorometric Index during the Winter Season in the Baltic Sea—The Case of the Gulf of Gdansk. *Sensors* **2022**, *22*, 6014. [CrossRef]
12. Williamson, C.E.; Saros, J.E.; Vincent, W.F.; Smol, J.P. Lakes and reservoirs as sentinels, integrators, and regulators of climate change. *Limnol. Oceanogr.* **2009**, *54*, 2273–2282. [CrossRef]
13. Tranvik, L.J.; Downing, J.A.; Cotner, J.B.; Loiselle, S.A.; Striegl, R.G.; Ballatore, T.J.; Dillon, P.; Finlay, K.; Fortino, K.; Knoll, L.B.; et al. Lakes and impoundments as regulators of carbon cycling and climate. *Limnol. Oceanogr.* **2009**, *54*, 2298–2314. [CrossRef]
14. Ficek, D. *The Bio-Optical Properties of Pomeranian Lakes and Their Comparison with the Properties of Other Lakes and the Baltic*; Institute of Oceanology Polish Academy of Sciences: Sopot, Poland, 2013; pp. 1–351.
15. Deutsch, E.S.; Cardille, J.A.; Koll-Egyed, T.; Fortin, M.-J. Landsat 8 Lake Water Clarity Empirical Algorithms: Large-Scale Calibration and Validation Using Government and Citizen Science Data from across Canada. *Remote Sens.* **2021**, *13*, 1257. [CrossRef]
16. Soomets, T.; Uudeberg, K.; Jakovels, D.; Brauns, A.; Zagars, M.; Kutser, T. Validation and Comparison of Water Quality Products in Baltic Lakes Using Sentinel-2 MSI and Sentinel-3 OLCI Data. *Sensors* **2020**, *20*, 742. [CrossRef]
17. Ogashawara, I.; Mishra, D.R.; Gitelson, A.A. Remote Sensing of Inland Waters: Background and Current State-of-the-Art. In *Bio-Optical Modeling and Remote Sensing of Inland Waters*; Mishra, D.R., Ogashawara, I., Gitelson, A.A., Eds.; Elsevier Inc.: Amsterdam, The Netherlands, 2017; pp. 1–24.
18. Miller, R.L.; Del Castillo, C.E.; McKee, B.A. *Remote Sensing of Coastal Aquatic Environments*; Springer: Dordrecht, The Netherlands, 2010; pp. 1–346.
19. Lednicka, B.; Otremba, Z.; Piskozub, J. Light Penetrating the Seawater Column as the Indicator of Oil Suspension-Monte Carlo Modelling for the Case of the Southern Baltic Sea. *Sensors* **2023**, *23*, 1175. [CrossRef] [PubMed]
20. Seegers, B.N.; Werdell, P.J.; Vandermeulen, R.A.; Salls, W.; Stumpf, R.P.; Schaeffer, B.A.; Owens, T.J.; Bailey, S.W.; Scott, J.P.; Lofti, K.A. Satellites for long-term monitoring of inland US lakes: The MERIS time series and application for chlorophyll-a. *Remote Sens. Environ.* **2021**, *266*, 112665. [CrossRef]
21. IOCCG. *Synergy between Ocean Colour and Biogeochemical/Ecosystem Models*; Dutkiewicz, S., Ed.; IOCCG Report Series, No. 19; International Ocean Colour Coordinating Group: Dartmouth, NS, Canada, 2020. [CrossRef]
22. Lednicka, B.; Kubacka, M. Semi-empirical model of remote-sensing reflectance for chosen areas of the southern Baltic. *Sensors* **2022**, *22*, 1105. [CrossRef]
23. Gordon, H.R.; Brown, O.B.; Evans, R.H.; Brown, J.W.; Smith, R.C.; Baker, K.S.; Clark, D.K. A semianalytic radiance model of ocean color. *J. Geophys. Res.* **1988**, *93*, 10909–10924. [CrossRef]
24. Carder, K.L.; Chen, F.R.; Lee, Z.P.; Hawes, S.K.; Kamykowski, D. Semi-analytic Moderate-Resolution Imaging Spectrometer algorithms for chlorophyll a and absorption with bio-optical domains based on nitrate-depletion temperatures. *J. Geophys. Res.* **1999**, *104*, 5403–5422. [CrossRef]
25. Maritorena, S.; Siegel, D.A.; Peterson, A. Optimization of a semi-analytical ocean color model for global scale applications. *Appl. Opt.* **2002**, *41*, 2705–2714. [CrossRef]
26. Majchrowski, R.; Stoń-Egiert, J.; Ostrowska, M.; Woźniak, B.; Ficek, D.; Lednicka, B.; Dera, J. Remote sensing of vertical phytoplankton pigment distributions in the Baltic: New mathematical expressions. Part 2: Accessory pigment distribution. *Oceanologia* **2007**, *49*, 491–511.
27. Woźniak, S.B.; Meler, J.; Lednicka, B.; Zdun, A.; Stoń-Egiert, J. Inherent optical properties of suspended particulate matter in the southern Baltic Sea. *Oceanologia* **2011**, *53*, 691–729.

28. Meler, J.; Kowalczuk, P.; Ostrowska, M.; Ficek, D.; Zabłocka, M.; Zdun, A. Parameterization of the light absorption properties of chromophoric dissolved organic matter in the Baltic Sea and Pomeranian lakes. *Ocean. Sci.* **2016**, *12*, 1013–1032. [CrossRef]
29. Wang, G.; Lee, Z.; Mouw, C. Multi-Spectral Remote Sensing of Phytoplankton Pigment Absorption Properties in Cyanobacteria Bloom Waters: A Regional Example in the Western Basin of Lake Erie. *Remote Sens.* **2017**, *9*, 1309. [CrossRef]
30. Odermatt, D.; Gitelson, A.; Brando, V.E.; Schaepman, M. Review of constituent retrieval in optically deep and complex waters from satellite imagery. *Remote Sens. Environ.* **2012**, *118*, 116–126. [CrossRef]
31. Malthus, T.J.; Lehmann, E.; Ho, X.; Botha, E.; Anstee, J. Implementation of a satellite based inland water algal bloom alerting system using analysis ready data. *Remote Sens.* **2019**, *11*, 2954. [CrossRef]
32. Sagan, V.; Peterson, K.T.; Maimaitijiang, M.; Sidike, P.; Sloan, J.; Greeling, B.A.; Maalouf, S.; Adams, C. Monitoring inland water quality using remote sensing: Potential and limitations of spectral indices, bio-optical simulations, machine learning, and cloud computing. *Earth-Sci. Rev.* **2020**, *205*, 103187. [CrossRef]
33. Bresciani, M.; Giardino, C.; Fabbretto, A.; Pellegrino, A.; Mangano, S.; Free, G.; Pinardi, M. Application of New Hyperspectral Sensors in the Remote Sensing of Aquatic Ecosystem Health: Exploiting PRISMA and DESIS for Four Italian Lakes. *Resources* **2022**, *11*, 8. [CrossRef]
34. Jiang, H.; Liu, Y.; Lu, J. A new algorithm for monitoring backflow from river to lake (BRL) using satellite images: A case of Poyang Lake, China. *Water* **2021**, *13*, 1166. [CrossRef]
35. Morel, A. Optical properties of pure water and pure sea water. In *Optical Aspects of Oceanography*; Jerlov, N.G., Nielsen, E.S., Eds.; Academic Pres: New York, NY, USA, 1974; pp. 1–24.
36. Smith, R.C.; Baker, K.S. Optical properties of the clearest natural waters (200–800 nm). *Appl. Opt.* **1981**, *20*, 177–184. [CrossRef]
37. Baranowski, D.; Chlost, I. Baltic Coastal Zone. *J. Ecol. Prot. Coastline* **2009**, *13*, 109–119.
38. Ficek, D.; Zapadka, T.; Dera, J. Remote sensing reflectance of Pomeranian lakes and the Baltic. *Oceanologia* **2011**, *53*, 959–970. [CrossRef]
39. Pápista, É.; Ács, É.; Böddi, B. Chlorophyll-a determination with ethanol—A critical test. *Hydrobiologia* **2002**, *485*, 191–198. [CrossRef]
40. Woźniak, S.B.; Darecki, M.; Zabłocka, M.; Burska, D.; Dera, J. New simple statistical formulas for estimating surface concentrations of suspended particulate matter (SPM) and particulate organic carbon (POC) from remote-sensing reflectance in the southernBaltic Sea. *Oceanologia* **2016**, *58*, 161–175. [CrossRef]
41. Stoń, J.; Kosakowska, A. Phytoplankton pigments designation—An application of RP-HPLC in qualitative and quantitative analysis. *J. Appl. Phycol.* **2002**, *14*, 205–210. [CrossRef]
42. Kowalczuk, P. The absorption of yellow substance in the Baltic Sea. *Oceanologia* **2002**, *44*, 287–288.
43. Nima, C.; Frette, Ø.; Hamre, B.; Stamnes, J.J.; Chen, Y.C.; Sørensen, K.; Norli, M.; Lu, D.; Xing, Q.; Muyimbwa, D.; et al. CDOM Absorption Properties of Natural Water Bodies along Extreme Environmental Gradients. *Water* **2019**, *11*, 1988. [CrossRef]
44. Morel, A.; Gentili, B. Diffuse reflectance of oceanic waters. III. Implication of bidirectionality for the remote-sensing problem. *Appl. Opt.* **1996**, *35*, 4850–4862. [CrossRef]
45. Zhang, Y.; Liu, M.; Qin, B.; van der Woerd, H.J.; Li, J.; Li, Y. Modeling Remote-Sensing Reflectance and Retrieving Chlorophyll-a Concentration in Extremely Turbid Case-2 Waters (Lake Taihu, China). *IEEE Trans. Geosci. Remote Sens.* **2009**, *47*, 1937–1948. [CrossRef]
46. Woźniak, B.; Dera, J. *Light Absorption in Sea Water*; Springer: New York, NY, USA, 2007; pp. 1–452.
47. Saiyidah Munirah, M.H.; Jafar-Sidik, M.; Nurzaliah, A.; Chen, C.-A.; Robert, J.W.B.; Suffian, I.; Noir, P.P. Dynamics of absorption properties of CDOM and its composition in Likas estuary, North Borneo, Malaysia. *Oceanologia* **2022**, *64*, 583–594.
48. Xue, K.; Ma, R.; Wang, D.; Shen, M. Optical Classification of the Remote Sensing Reflectance and Its Application in Deriving the Specific Phytoplankton Absorption in Optically Complex Lakes. *Remote Sens.* **2019**, *11*, 184. [CrossRef]
49. Effler, S.W.; Peng, F.; O'Donnell, D.M.; Strait, C. The backscattering coefficient and its components in the Great Lakes: A review and synthesis. *J. Great Lakes Res.* **2013**, *39*, 108–122. [CrossRef]
50. Guofeng, W.; Lijuan, C.; Hongtao, D.; Teng, F.; Yaolin, L. Absorption and backscattering coefficients and their relations to water constituents of Poyang Lake, China. *Appl. Opt.* **2011**, *50*, 6358–6368.
51. Kutser, T.; Hiire, M.; Metsamaa, L.; Vahtmäe, E.; Paavel, B.; Aps, R. Field measurements of spectral backscattering coefficient of the Baltic Sea and boreal lakes. *Boreal Environ. Res.* **2009**, *14*, 305–312.